Journal of Electrical and Computer Engineering Innovations
(JECEI)
Journal homepage: http://www.jecei.sru.ac.ir

Research paper

Enhancement of the Photoresponse in the Platinum Silicide Photodetector by a Graphene Layer

A.H. Mehrfar, A. Eslami Majd*

Faculty of Electrical and Computer Engineering, Malek Ashtar University of Technology, Tehran, Iran.

Article Info

Article History:
Received 15 November 2021
Reviewed 21 December 2021
Revised 02 February 2022
Accepted 05 February 2022

Keywords:
Two-dimensional
Near-infrared
Optoelectronic

*Corresponding Author's Email Address:
a_eslamimajd@mut-es.ac.ir

Abstract

Background and Objectives: The use of two-dimensional materials in the photodetector fabrication has received much attention in recent years. Graphene is a two-dimensional material that has been extensively researched to make photodetectors. The responsivity of graphene photodetectors was limited by the low optical absorption in graphene (~2.3% for single layer graphene). Therefore, graphene along with other materials has been used to fabricate a photodetector with the desired properties. The graphene is used for the improvement of the silicide platinum photodetector.

Methods: The platinum silicide photodetector with graphene has been experimentally fabricated and characterized, and all steps of the device fabrication and the characterization are completely provided in addition to required equations for device analysis is completely provided. A graphene layer is transferred on the platinum silicide layer, and the graphene layer creates the photoconductor gain in the platinum silicide photodetector.

Results: In the proposed device, near-infrared light is detected in the platinum silicide, and by placing a layer of graphene on the platinum silicide, the optical current and responsivity increase compared to the platinum silicide photodetector without graphene. Experimental results show that the optical current, external quantum efficiency, and responsivity increase in the platinum silicide photodetector with graphene. The graphene not only functions as the charge transport channel, but also works as a photoconductor.

Conclusion: The optical current and responsivity are increased by the platinum silicide photodetector with graphene. In our photodetector, the highest responsivity is 120 $\frac{mA}{W}$ in the 1310 nm wavelength, and the optical current is 100 nA at the applied voltage of 8 V. Our photodetector has optical current, responsivity, and external quantum efficiency twice as much as platinum silicide photodetector. Experimental results show the good performance of graphene with platinum silicide photodetector.

Introduction

Graphene that is a two-dimensional material of carbon atoms is very attractive for optoelectronic applications [1]. Graphene has unique properties in mobility, conductivity, optical, and mechanical [1]-[4].

Graphene has a high photodetection potential due to its high speed and broad absorption spectrum [5]-[7]. Graphene can be an infrared photodetector operating at the room temperature. Graphene has potential

applications in mid-IR spectroscopy [8]-[10] and biochemical sensing [11].

The responsivity of graphene photodetectors was limited by the low optical absorption in graphene (~2.3% for single layer graphene) and short carrier life time (few picoseconds) [6]-[12]. To compensate the low responsivity of graphene photodetectors, recent research has focused on the enhancement of the responsivity of graphene photodetecors. For example by using metallic plasmonics [13], [14], a waveguide [15], quantum dots [16]-[18], and microcavities [19], responsivity increases in the graphene photodetector. However, there are problems that the photodetector speed decreases with increasing the responsivity; we can refer to the structures that have high responsivity using adsorbent layer or quantum dots, but the speed of the photodetectors is reduced due to the trapping of the carriers in the absorbent material or quantum dots [16], [20]. The graphene photodetector was reported with small metal antenna structures that can be designed to improve both light absorption and photocarrier collection in graphene photodetectors [21]. The Graphene/silicon Schottky photodetector based on internal photoemission effect was reported [22]. There are several problems that limit the practical applications of graphene photodetectors such as low responsivity, the high dark current, and difficult manufacturing steps [22]. On the other hand, Schottky photodetectors based on an internal photoemission effect emit carriers from the metal layer to the semiconductor. These types of photodetectors can be used in different wavelengths. One of the Schottky photodetectors is platinum silicide (PtSi) photodetectors for the photodetection of the infrared wavelength. Platinum silicide photodetectors have many advantages including simple manufacturing process, high stability, high speed, low costs. However, because only a small fraction of the carriers are transferred to the semiconductor, low quantum efficiency was reported for these photodetectors [20]. Therefore, the design and the fabrication of a photodetector that can reduce the problems of graphene photodetectors and platinum silicide photodetectors is very attractive.

In this paper, we have experimentally investigated a silicide platinum photodetector with graphene, and the proposed device is fabricated and characterized. In addition, required equations are provided for the device analysis. A graphene layer is transferred on the platinum silicide layer. The Schottky barrier of silicon and platinum silicide is used as a photodetector by the internal photoemission effect, and the graphene layer is used as a charge transport of excited carriers. By radiating laser light on the proposed device, the electron-hole pair is created in the platinum silicide. By applying an external electrical voltage to the device, one of the carriers travels through silicon and another carrier travels through the graphene, and electrical current is created. The optical current, external quantum efficiency and responsivity are increased by proposed device. Our photodetector has optical current, responsivity, and external quantum efficiency twice as much as platinum silicon photodetector.

Fabrication Process

The fabrication process of the platinum silicide photodetector with graphene is shown in Fig. 1. N-type silicon with 8 to 10 Ω.cm resistivity is used. In addition, for n-type silicon and platinum silicide, the height of the Schottky barrier is approximately 0.84 eV. This Schottky barrier has detection up to a wavelength of 1470 nm. If p-type silicon is used, the height of the schottky barrier is approximately 0.3 eV, and this Schottky barrier has detection up to a wavelength of 4100 nm. P-type silicon has detection in the higher wavelength, but a platinum silicide photodetector with p-type silicon can't operate at the room temperature. Therefore, the choice of the lightly doped n-type silicon is a good choice for a detector operating at the room temperature.

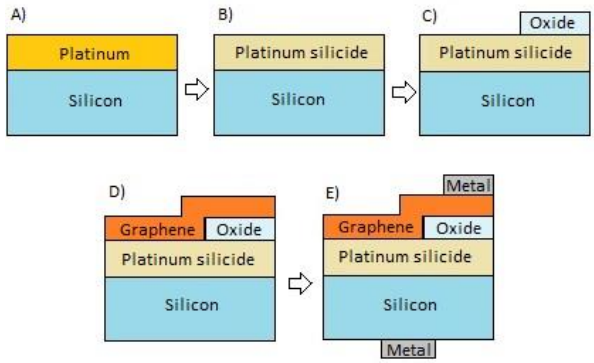

Fig. 1: The fabrication process of the platinum silicide photodetector with graphene.

The silicon surface must be clean. Therefore, the silicon surface is completely cleaned by RCA method. In the next step, a layer of platinum is deposited on the silicon by electron beam physical vapor deposition as shown in Fig. 1(A). After the deposition of the platinum layer, the sample is placed at 450 °C for one hour in the high vacuum (10^{-6} torr).

The formation of platinum silicide is illustrated in Fig. 2. The initial phase of a Pt_2Si layer begins to form at an interface layer, and silicon diffuses into platinum as shown in Fig. 2(B). Over time, the whole layer turns to Pt_2Si. The second phase of a platinum silicide layer is formed at the interface layer as shown in Fig. 2(D). At the end, the whole layer turns to platinum silicide as shown in Fig. 2(E).

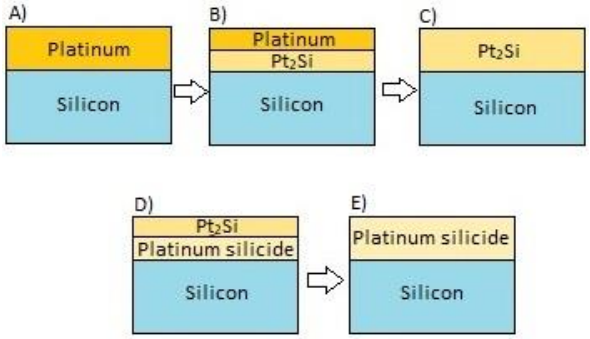

Fig. 2: The fabrication process of the platinum silicide.

Platinum silicide on the substrate is illustrated in Fig. 1(B). After the formation of the platinum silicide layer, the silicon oxide must be deposited on the platinum silicide. Therefore, the silicon oxide is deposited by sputtering with 150 nm thickness. The deposition is done by a shadow mask because the layer can be placed on the desired location as shown in Fig. 1 (C).

The real sample after the deposition of the silicon oxide is illustrated in Fig. 3. The location of silicon oxide and platinum silicide are also illustrated in Fig. 3.

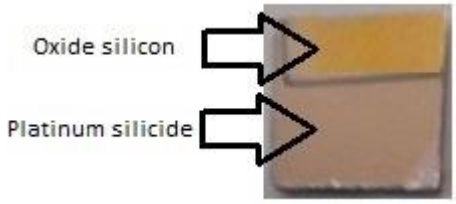

Fig. 3: A fabricated sample image after the deposition of the silicon oxide.

Graphene should be placed on the surface. In this structure, graphene grown by chemical vapor deposition method produced by Graphena Company is used. The graphene grown on copper as a single layer is illustrated in Fig. 4.

Fig. 4: Sample image of graphene on copper.

The graphene layer is a two-dimensional layer and is very thin, and this layer is not visible on a copper [23]. A PMMA layer that is used to protect and transfer is deposited on the graphene layer.

There are several ways to transfer graphene on different substrates. The most important of these methods include wet and dry. Among these methods, the wet method has more desirable properties, and it is more economical [24]. Therefore, a wet method is used to transfer graphene on the platinum silicide substrate. The transfer steps of the graphene by the wet method are illustrated in Fig. 5.

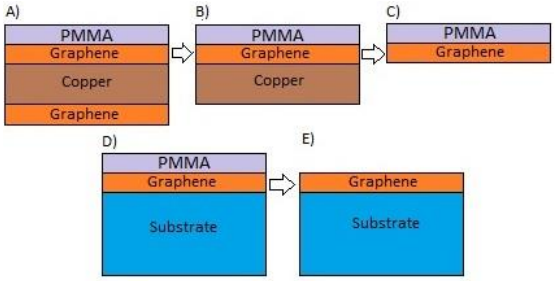

Fig. 5: Graphene transfer steps on the substrate.

The graphene on the copper from the side view is illustrated in Fig. 5(A).

There is a PMMA layer on the graphene, and there is graphene on the copper and under the copper. The graphene under the copper is not desirable and should be removed. Therefore, the sample is placed in dilute nitric acid solution to remove the graphene under the copper. Fig. 5(B) shows the sample after removing the graphene under the copper. In the next step, the sample is taken out from the nitric acid solution and the sample is rinsed by DI water. The sample is placed into an iron nitrate solution that has the suitable concentration to remove copper. Fig. 5(C) shows the sample after copper etching. After removing the copper, several rinsing steps are performed with DI water to eliminate completely the metal contamination. In the next step after cleaning the substrate surface with acetone, while the graphene sample is suspended on the water, the graphene is slowly placed on the substrate. The graphene on the substrate is shown in Fig. 5(D).

In the last step, after several annealing steps for graphene adhesion to the substrate, NMP solution is used to remove PMMA. Fig. 5(E) shows graphene on the substrate after PMMA etching.

Fig. 1(D) shows graphene on the platinum silicide and silicon oxide. Finally, metal contacts on the graphene and under silicon is deposited as shown in Fig. 1(E).

Theoretical Equations

Fig. 6 shows the energy band diagram of the graphene/PtSi/silicon structure. The incident photons are absorbed in the platinum silicide and generate electron-hole pairs. By applying a voltage between two metal contacts, the excited electrons randomly walk in the platinum silicide layer until they reach the interface between the platinum silicide and the silicon. The electrons surmount the barrier and are emitted into the silicon [20]. The generated holes move to a negative voltage that is connected to the metal contact on the graphene.

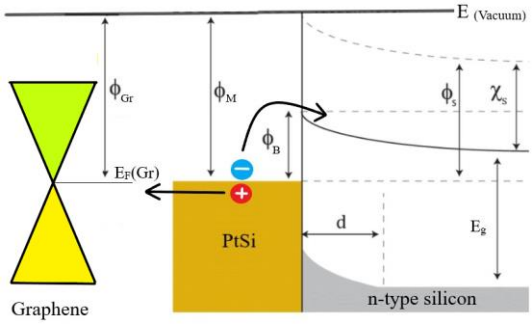

Fig. 6: The energy band diagram of the graphene/PtSi/silicon structure.

Fig.7 shows a side view of the structure to analyze the device. As shown in Fig. 7, an external voltage is applied to two metal contacts that are placed under the silicon and on the graphene that is placed on the silicon oxide. By applying an external voltage, the created electron-hole pair separates from each other and moves towards the metal contacts. In Fig. 7, the electron is shown in a black color and is moved towards the positive voltage, and its path to the metal contact under the silicon is shown with black arrows. The hole is shown in a white color and is moved towards the negative voltage, and its path from inside the graphene to the metal contact on the graphene is shown with white arrows. By applying an external voltage, the excited hole and electron are separated from each other and take two separate paths.

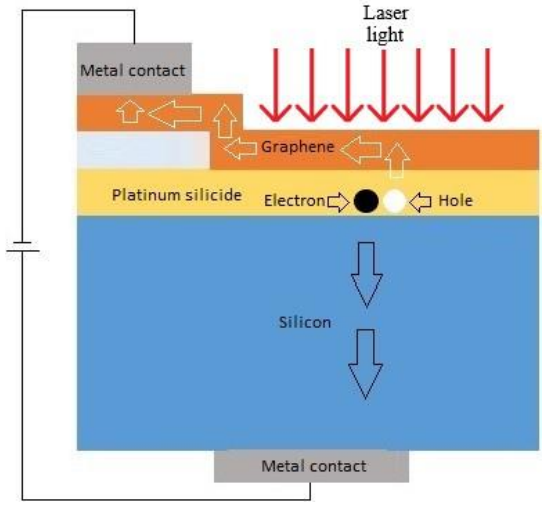

Fig. 7: The movement path of electrons and holes inside the structure after a laser radiation.

The electron travels vertically through the silicon, and the hole travels horizontally through the graphene. Because the mobility graphene is higher than silicon, holes reach the metal contact faster than electrons. The remained electrons cause extra holes to be injected into the device by external voltage, and more photocurrent is created. The graphene not only functions as the charge transport channel, but also works as a photoconductor [25].

The modified Fowler theory is an equation for the estimation of the internal quantum efficiency of Schottky photodetctors given by [26]-[30]:

$$\eta = \frac{1}{8\phi b}\frac{(hv-\phi b)^2}{hv} \quad (1)$$

where h is plank constant, v is the frequency of the incident infrared light and ϕ_b is the Schottky barrier height of the platinum silicide and silicon. Equation (1) describes the internal quantum efficiency that is the number of photo-carriers collected by the photdetectors to the number of photons absorbed by the photodetector. Obviously, η depends on the incident photon energy and the Schottky barrier height.

The basic expression describing photocurrent in the photodetector is [25]:

$$\mathrm{I} = \alpha \times \varphi \times G \times e \times \eta \quad (2)$$

where α is the adsorption rate of photodetector, φ is the incident photon flux, G is the photoconductive gain, and e is electron charge. The incident photon flux, φ, rate can be determined by the total optical power per photon energy [22]:

$$\varphi = \frac{\rho \times Wg \times Lg}{hv} \quad (3)$$

where ρ is incident IR power density, W_g is the width of the channel, and L_g is the length of the channel. The photoconductive gain, G, is determined by the properties of the photodetector. The photoconductive gain can be defined as the number of carriers passing contacts per generated pair. The photoconductive gain is expressed by [25]:

$$G = \frac{\tau}{Tr} \quad (4)$$

where τ is the recombination time and Tr is the transit time in the graphene channel. Tr is expressed by [25]:

$$\mathrm{Tr} = \frac{L^2}{\mu \times V} \quad (5)$$

where L is the length of the graphene channel that generated carriers travel, μ is the mobility graphene, and V is applied voltage. The photoconductive gain for the high-quality graphene with the mobility of $1 \times 10^4 \frac{cm^2}{V.S}$, the 100 μm channel length, and 5 V bias voltage is less than one because the ultrafast photo-induced carrier recombination time in the graphene is in picosecond range. On the contrary, the photo-induced carriers are separated by the platinum silicide/silicon in our device, resulting in a much longer recombination time.

Results and Discussion

One of the best ways to measure graphene coverage on a surface is to take SEM images. Therefore, after graphene is transferred on the substrate, good informations can be obtained by taking the SEM image of graphene. Fig. 8 shows the SEM image of the graphene on the platinum silicide and silicon oxide substrate.

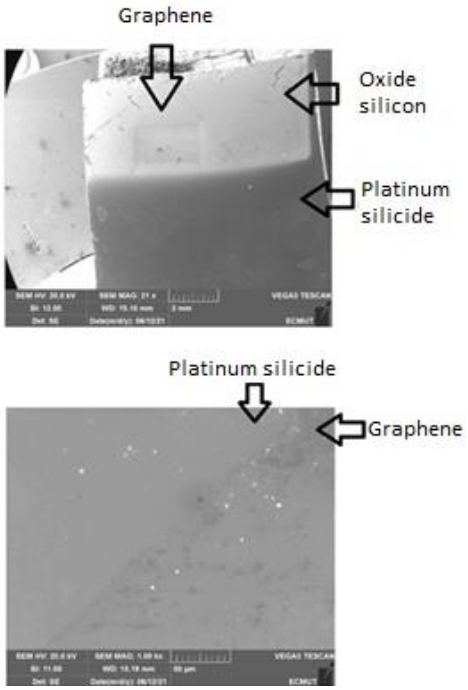

Fig. 8: SEM image of graphene on the surface of the platinum silicide.

SEM images were taken by the TESCAN VEGA3 tool. Fig. 8(A) shows the SEM image of the graphene on a surface with a magnification of 21. The part of the graphene is on the silicon oxide and another part on the platinum silicide. The silicon oxide in the image is shiny, and the platinum silicide is dark. The graphene has a very small thickness and does not have a specific color. The location of the graphene is shown by lines of the graphene edge. Fig. 8(B) shows the SEM image with magnification of 1000. This image is taken from the location of graphene on the surface of the platinum silicide. In the SEM images, the PMMA layer is removed from the graphene.

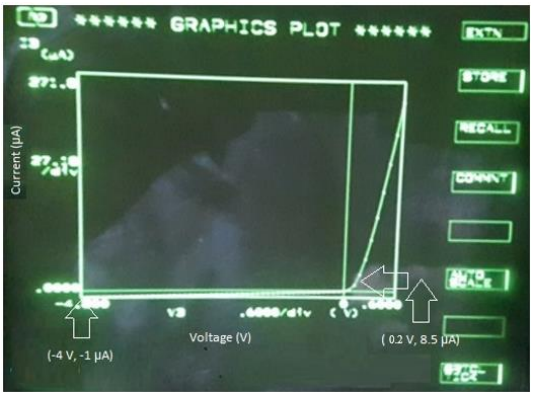

Fig. 9: I-V characteristic curve of Schottky diode between silicon and platinum silicide.

A Schottky diode is formed between silicon and platinum silicide. As shown in Fig. 9, I–V curve was obtained by an HP4450 semiconductor measurement device. To draw this curve, one terminal is connected to silicon and another terminal to platinum silicide. A sweep voltage from -4 to +0.6 V is applied to the platinum silicide, and the silicon is connected to a ground.

The Schottky diode is formed between silicon and platinum silicide. The diode anode is on the platinum silicide side, and the diode cathode is on the silicon side. The results are as expected; because n-type silicon is used, the silicon must act as a cathode for a Schottky diode. The characteristic curve of the diode I-V is theoretically obtained by [20]:

$$I = ABT^2 e^{\frac{-q\phi b}{kT}} \left(e^{\frac{qv}{nkT}} - 1\right) \quad (6)$$

where A is the junction area, B is the Richardson constant, ϕ_b is the height of the Schottky barrier, k is Boltzmann constant, and T is the absolute temperature [20]. To characterize the photodetector, a wavelength of less than 1470 nm must be applied to the photodetector. The wavelength should not be in the visible range because silicon has a high absorption in in this range and produces a lot of optical current. For this reason, the detection of the Schottky photodetector of platinum silicide is not observed. Therefore, the wavelength should be greater than the visible range and less than 1470 nm. A good choice for the optical test of the photodetector is the use of a laser with a 1310 nm wavelength, which can show the detection of platinum silicide photodetector. By radiating laser light, the electron-hole pairs are created in the platinum silicide. By applying an external voltage, the carriers separate from each other and move towards the metal contacts. To calculate the optical current and responsivity of the photodetector, an optical setup must be prepared to minimize environment noise and to calculate the amount of optical current and responsivity. For this reason, an optical setup is prepared as shown in Fig. 10.

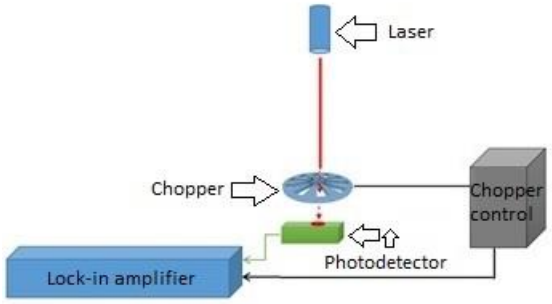

Fig. 10: Optical setup of the photodetector test.

In this optical setup, the 1310 nm wavelength is continuously radiated by the laser. After the light passes through a chopper with a 3 kHz frequency, the light is discrete and reaches to the photodetector. The laser spot diameter is 500 μm, and the laser power that reaches to the photodetector is 8.5 μW. Because the laser light reaches the photodetector discretely, the electrical current generated by the photodetector is discrete. The photodetector output and the chopper reference output are connected to a lock-in amplifier. In the lock-in amplifier, after electrical signals pass through

various circuits, including frequency multiplier, Integrator circuit, amplifier, etc., the desired output is achieved with minimal noise.

There are two advantages at this optical setup; the first advantage is in reducing the environment noise, and the second advantage is in detection of the smallest electrical current. The current output from the photodetector includes the dark current and the optical current. The dark current is the current that passes through the photodetector in reverse bias without applying light. By applying laser light, the optical current is generated by the photodetector. If the dark current is subtracted from the photodetector output current, optical current is obtained [20]:

$$Iph = I(t) - I(dark) \quad (7)$$

where $I_{(t)}$ is the photodetector output current, $I_{(dark)}$ is the dark current, and I_{ph} is the optical current. The responsivity rate in terms of A/W for the photodetector is obtained [20]:

$$R = \frac{I_{ph}}{P} \quad (8)$$

where I_{ph} is the optical current, and P is the input power. External quantum efficiency of the photodetecor is given by [20]:

$$QE_{ex} = \frac{R}{\lambda} \times 1.245 \quad (9)$$

where R is responsivity, and λ is infrared wavelength. The fabricated photodetector is characterized in different ways. This photodetector is characterized by two cases of the platinum silicide photodetector with graphene and the platinum silicide photodetector without graphene. In the first case, the laser light is radiated on where the graphene is placed on the platinum silicide. The first case is shown in Fig. 11(A).

In the second case, the laser light is radiated on where platinum silicide is present, and there is no graphene. The second case is shown in Fig. 11(B). In this case, the platinum silicide photodetector works without graphene. In both cases, the contact must be taken from the structure to apply electrical voltage. In the first case, a contact is connected to silicon and another contact is connected to graphene on the silicon oxide. In the second case, the contact is connected to the platinum silicide, and another contact is connected to silicon.

In the Fig. 12, the optical current and the output voltage of the lock-in amplifier under different voltages are illustrated for both cases platinum silicide photodetector with graphene and platinum silicide photodetector without graphene. A resistor that help to calculation of the optical current is connected to photodetector in series.

After calculation of the optical current, responsivity is calculated by (8). In the Fig. 13, responisivity in different voltage are illustrated for both cases platinum silicide photodetector with graphene and platinum silicide photodetector without graphene.

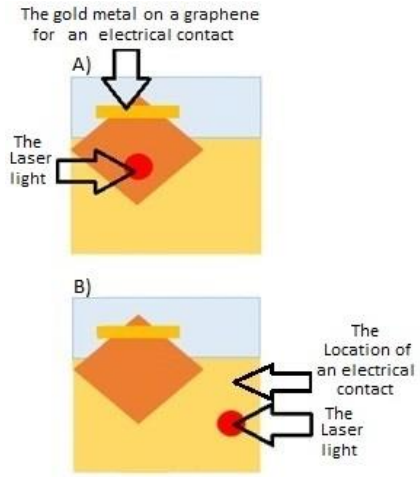

Fig. 11: Location of laser light in different cases.

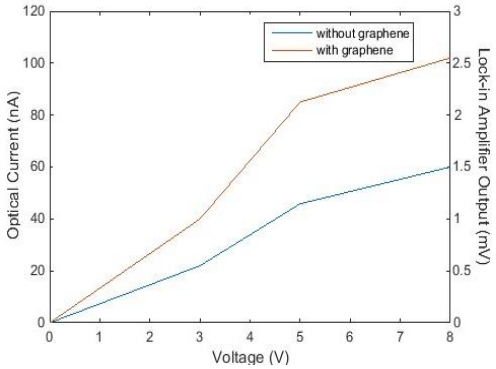

Fig. 12: The optical current and the output voltage of the lock-in amplifier under different voltages.

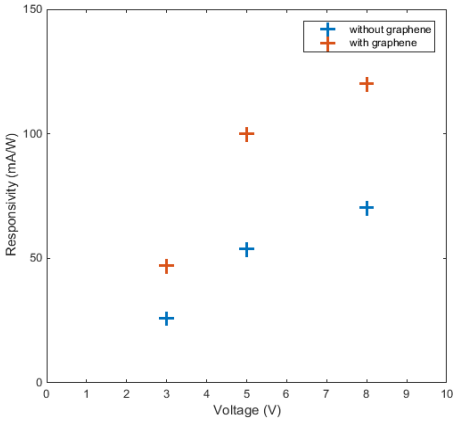

Fig. 13: photodetector responsivity under different voltages.

External quantum efficiency is calculated by (9). In the Fig. 14, external quantum efficiency in different voltage are illustrated for both cases platinum silicide photodetector with graphene and platinum silicide photodetector without graphene.

The platinum silicide photodetector with graphene has more optical current, responsivity, and external quantum efficiency than platinum silicon photodetector without graphene. In Table 1, our device is compared by several photodetectors previously reported. The use of

graphene with platinum silicon has very interesting properties that can be considered in the future.

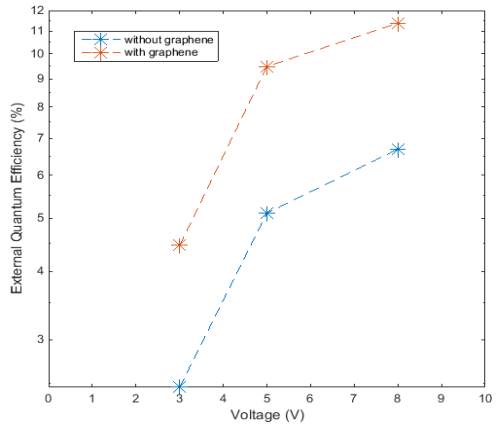

Fig. 14: External quantum efficiency of the photodetector under different voltages.

Table. 1: Summary of responsivity of several photodetectors previously reported

Structure	Responsivity	Wavelength	Ref
Platinum silicide with graphene	120 mA/W	1310 nm	This work
Platinum silicide	52 mA/W	1550 nm	[20]
Graphene	6.1 mA/W	1550 nm	[6]
Graphene/ silicon hetrostructure	2.29 mA/W	1550 nm	[22]
Graphene with cavity	20 mA/W	850 nm	[19]

Conclusion

In this paper, a photdetector structure of platinum silicide with graphene is presented. A graphene layer is placed on the platinum silicide. By radiating laser light, the electron-hole pairs are created in the platinum silicide. The photo-induced carriers separate from each other and move towards the metal contacts. The generated holes travel through the graphene and the generated electrons travels through the silicon. Because the mobility graphene is higher than silicon, holes reach the metal contact faster than electrons. The graphene not only functions as the charge transport channel, but also works as a photoconductor. Our device has more optical current, responsivity, and external quantum efficiency than platinum silicon photodetector. In our photodetector, the highest responsivity is 120 $\frac{mA}{W}$ in the 1310 nm wavelength, and the optical current is 100 nA at the applied voltage of 8 V. Our photodetector has optical current, responsivity, and external quantum efficiency twice as much as platinum silicide photodetector. This device can be a good candidate for optical communication applications.

Author Contributions

A.H. Mehrfar and A. Eslami Majd designed the experiments and collected the data. A. H. Mehrfar wrote the manuscript.

Acknowledgment

The authors would like to acknowledge the Faculty of Electrical & Computer Engineering, Malek Ashtar University of Technology, and the Microelectronic laboratory, for their support and contribution to this study.

Conflict of Interest

The authors declare no potential conflict of interest regarding the publication of this work. In addition, the ethical issues including plagiarism, informed consent, misconduct, data fabrication and, or falsification, double publication and, or submission, and redundancy have been completely witnessed by the authors.

Abbreviations

PtSi	Platinum Silicide
PMMA	poly methyl methacrylate
NMP	N-Methyl-2-Pyrrolidone
SEM	Surface Imaging Method

References

[1] F. Bonaccorso, Z. Sun, T. Hasan, A.C. Ferrari, “Graphene photonics and optoelectronics,” Nat. photonics, 4(9): 611-622, 2010.

[2] R.R. Nair, P. Blake, A.N. Grigorenko, K.S. Novoselov, T. J. Booth, et al., “Fine structure constant defines visual transparency of graphene,” Science, 320(5881): 1308, 2008.

[3] K.I. Bolotin, K.J. Sikes, Z. Jiang, M. Klima, G. Fudenberg, et al., “Ultrahigh electron mobility in suspended graphene,” Solid state commun., 146(9): 351-355, 2008.

[4] V. Singh, D. Joung, L. Zhai, S. Das, S.I. Khondaker, et al., “Graphene based materials: past, present and future,” Prog. Mater. Scie., 56(8): 1178–1271, 2011.

[5] A.K. Geim, K.S. Novoselov, “The rise of graphene, in Nanoscience and technology: a collection of reviews from nature journals,” World Scientific, 11-19, 2010.

[6] T. Mueller, F. Xia, and P. Avouris, “Graphene photodetectors for high-speed optical communications,” Nat. photonics, 4(5): 297-301, 2010.

[7] F. Xia, T. Mueller, Y. Lin, A. Valdes-Garcia, and P. Avouris “Ultrafast Graphene Photodetector,” Nat. Nanotechnol., 4(12):839, 2009.

[8] B. Guo, Y. Wang, C. Peng, H.L. Zhang, G.P. Luo, et al., “Laser-based mid-infrared reflectance imaging of biological tissues,” Opt. express, 12(1): 208–219, 2004.

[9] C. Young, S.S. Kim, Y. Luzinova, M. Weida, D. Arnone, et al., “External cavity widely tunable quantum cascade laser based hollow waveguide gas sensors for multianalyte detection,” Sens. Actuators B, 140(1): 24–28, 2009.

[10] S. Cakmakyapan, P.K. Lu, A. Navabi, M. Jarrahi, “Gold-patched graphene nano-stripes for high-responsivity and ultrafast photodetection from the visible to infrared regime,” Light Sci. Appl., 7(1):20, 2018.

[11] A.B. Seddon, “Mid-infrared (IR)–A hot topic: The potential for using mid-IR light for non-invasive early detection of skin cancer in vivo,” phys. status solidi B, 250(5), 1020–1027 2013.

[12] J.M. Dawlaty, S. Shivaraman, M. Chandrashekhar, F. Rana, M.G. Spencer, “Measurement of ultrafast carrier dynamics in epitaxial graphene,” Appl. Phys. Lett., 92(4): 42116-42118, 2008.

[13] T. Low, P. Avouris, “Graphene plasmonics for terahertz to mid-infrared applications,” ACS nano, 8(2): 1086-1101, 2014.

[14] T.J. Echtermeyer, L. Britnell, P.K. Jasnos, A. Lombardo, R.V Gorbachev, et al., “Strong plasmonic enhancement of photovoltage in graphene,” Nat. Commun., 2(1): 1–5, 2011.

[15] R.J. Shiue, Y. Gao, Y. Wang, C. Peng, A.D. Robertson, et al., "High-responsivity graphene–boron nitride photodetector and autocorrelator in a silicon photonic integrated circuit," Nano let., 15(11): 7288-7293, 2015.

[16] G. Konstantatos, M. Badioli, L. Gaudreau, J. Osmond, M. Bernechea, et al., "Hybrid graphene–quantum dot phototransistors with ultrahigh gain," Nat. nanotechnol., 7(6): 363-368, 2012.

[17] X. Tang, K.W.C. Lai, "Graphene/HgTe quantum-dot photodetectors with gate-tunable infrared response," ACS Appl. Nano Mater., 2(10): 6701–6706, 2019.

[18] Y. Chan, Z. Dahua, Y. Jun, T. Linlong, L. Chongqian, et al., "Fabrication of hybrid Graphene/CdS quantum dots film with the flexible photo-detecting performance," Physica E, 124: 114216, 2020.

[19] M. Furchi, A. Urich, A. Pospischil, G. Lilley, K. Unterrainer, et al., "Microcavity-integrated graphene photodetector," Nano let., 12(6): 2773–2777, 2012.

[20] A. Rogalski, Infrared and Terahertz Detectors, the third edition, CRC press, 2018.

[21] Y. Yao, R. Shankar, P. Rauter, Y. Song, J. Kong, et al., "High-responsivity mid-infrared graphene detectors with antenna-enhanced photocarrier generation and collection," Nano let., 14(7): 3749–3754, 2014.

[22] X. Tang, H. Zhang, X. Tang, K.W.C. Lai, "Photoresponse enhancement in graphene/silicon infrared detector by controlling photocarrier collection," Mater. Res. Express, 3(7): 76203-76214, 2016.

[23] A. Reina, X. Jia, J. Ho, D. Nezich, H. Son, et al., "Large area, few-layer graphene films on arbitrary substrates by chemical vapor deposition," Nano Lett., 9 (1): 30–35, 2009.

[24] J.W. Suk, A. Kitt, C.W. Magnuson, Y. Hao, S. Ahmed, et al., "Transfer of CVD-grown monolayer graphene onto arbitrary substrates", ACS nano, 5(9): 6916–6924, 2011.

[25] A. Rogalski, 2D materials for Infrared and Terahertz Detectors, the first edition, CRC press, 2020.

[26] J.M. Mooney, J. Silverman, "The theory of hot-electron photoemission in Schottky-barrier IR detectors," IEEE Trans. Electron devices, 32(1): 33–39, 1985.

[27] V.E. Vickers, "Model of schottky barrier hot-electron-mode photodetection," Appl. Opt., 10(9): 2190–92, 1971.

[28] V.L. Dalal, "Simple model for internal photoemission," J. Appl. Phys., 42(6): 2274–2279, 1971.

[29] Z. Chen, Z. Cheng, J. Wang, X. Wan, C. Shu, et al., "High responsivity, broadband, and fast graphene/silicon photodetector in photoconductor mode," Adv. Opt. Mater., 3(9): 1207–1214, 2015.

[30] M. Amirmazlaghani, F. Raissi, O. Habibpour, J. Vukusic, J. Stake, "Graphene-Si Schottky IR detector," IEEE J. Quantum Electron., 49(7): 589–94, 2013.

Biographies

Amir Hossein Mehrfar was born in Tehran, Iran, 1991. He received the B.Sc. degree in Electrical Engineering from the University of Ghiaseddin Jamshid Kashani, in 2013. He received the M.Sc. degree in Electrical Engineering from Islamic Azad University South Tehran Branch. He is currently a Ph.D. student in the Malek-Ashtar University of Technology, Tehran, Iran. His current research interests include Graphene-Based Optoelectronics, Design and Modeling of Nano-Scale Semiconductor Devices, Design and Fabrication of IR Detectors.

- Email: Mehrfar.a.h@mut.ac.ir
- ORCID: 0000-0002-0501-0991
- Web of Science Researcher ID: NA
- Scopus Author ID: NA
- Homepage: NA

Abdollah Eslami Majd was born in Hamadan, Iran, on March 23, 1976. He received the B.E. degree in applied physics from bu-ali Sina University, Hamadan, Iran in 1998. He received M.E. degree in atomic and molecular physics from Amir kabir University of Technology Tehran Polytechnic, Tehran, Iran in 2001. He received the Ph.D. Degree in photonics from laser and plasma Institute of Shahid Beheshti University, Tehran, Iran in 2011. Since joining electrical engineering and electronic department of Malek Ashtar University of Technology in 2012, he has engaged in research and development of stary light in the satellite camera, laser induced breakdown spectroscopy (LIBS) and hemispherical resonator gyroscope (HRG). He is co-author of more than 30 publications. Dr. Eslami is a member of Optics and Photonics Society of Iran and Physics Society of Iran.

- Email: a_eslamimajd@mut-es.ac.ir
- ORCID: 0000-0002-7538-3160
- Web of Science Researcher ID: NA
- Scopus Author ID: NA
- Homepage: NA

How to cite this paper:

A.H. Mehrfar, A. Eslami Majd, "Enhancement of the photoresponse in the platinum silicide photodetector by a graphene layer," J. Electr. Comput. Eng. Innovations, 10(2): 363-370, 2022.

DOI: 10.22061/JECEI.2022.8487.517

URL: https://jecei.sru.ac.ir/article_1676.html